

Full Length Research Paper

Hierarchical cluster analysis of hydrochemical data as a tool for assessing the evolution and dynamics of groundwater across the Ethiopian rift

Tenalem Ayenew^{1*}, Shimeles Fikre², Frank Wisotzky³, Molla Demlie⁴ and Stefan Wornlich³

¹Addis Ababa University, Department of Earth Sciences, P.O.Box 1176. Addis Ababa, Ethiopia.

²Arba Minch University, Department of Applied Geology. P.O.Box 21. Arba Minch, Ethiopia.

³Ruhr University of Bochum, Department of Applied Hydrogeology, Universitaetsstr.150, D-44801.Bochum, Germany.

⁴School of Geological Sciences, University of Kwazulu-Natal. Durban, South Africa.

Accepted January 9, 2009

The hydrochemical evolution and flow pattern of groundwater is analyzed in a complex closed rift basin on the basis of multivariate hierarchical statistical cluster analysis. The analysis was made on the basis of water samples collected from over 120 wells and limited surface waters. The result revealed dissimilar hydrochemical phases in the rift and highlands representing different groundwater flow regimes. Five groundwater zones with different hydrochemical facies were identified. Both the conventional hydrochemical and multivariate statistical analyses indicate that the central sector of the rift represents a complex groundwater system influenced by thermal waters and alkaline lakes. It also demonstrates that the close similarity of lakes and groundwater with high fluoride, sodium, Total Dissolved Solids (TDS) and pH. The waters associated with acidic volcanic rocks are characterized by a positive alkalinity residual of calcite. When they concentrate due to the effect of climate, the precipitation of calcite causes a decrease in the chemical activity of calcium and increase in alkalinity. These waters become NaHCO₃-dominated with distinctly different from highland systems characterized by Ca-MgHCO₃ type waters with low TDS. Alkaline waters are intimately linked to acidic volcanics while fresh waters are associated with dominantly basic volcanics. Waters with similar hydrochemical facies as highland waters are evident in local fractures of the rift floor. The zonation of hydrochemical facies on the basis of hierarchical cluster analysis indicates increase in ionic concentration and pH along the groundwater flow path.

Key words: Ethiopian rift, groundwater evolution, hierarchical cluster analysis, hydrochemistry, volcanic rocks.

INTRODUCTION

The Ethiopian rift consists of three major regions with distinct volcanic and tectonic characteristics representing different stages of rifting. These are the broadly rifted zone of south-western Ethiopia, the Main Ethiopian Rift (MER) of central Ethiopia, and the Afar Depression. The study area, which is known by the name Ziway-Shala Basin (ZSB), is located at the centre of the MER some 200 km south of the capital Addis Ababa. The MER is characterized by a complex nested natural lakes fed by

rivers and groundwater that originate from eastern and western highlands. Four major lakes occupy ancestral depressions of Plio-Pleistocene calderas at the centre of the basin (Gasse and Street, 1978; Gasse, 1980). The lakes vary significantly in size, depth, hydrochemistry and hydrogeological setting.

The presence of many lakes and geothermal fields within a complex rift attracted major geoscientific and limnological investigations since the second half of the 20th century. Many of the geoscientific investigations related to hydrogeology and hydrochemistry revealed the importance of water-rock interactions in influencing the water quality in different parts of the Ethiopian rift and adjacent escarpments (Craig et al., 1977; Teklehaimanot

*Corresponding author. E-mail: Tenalema@yahoo.com.
Tel/Fax: 251-1112239462.

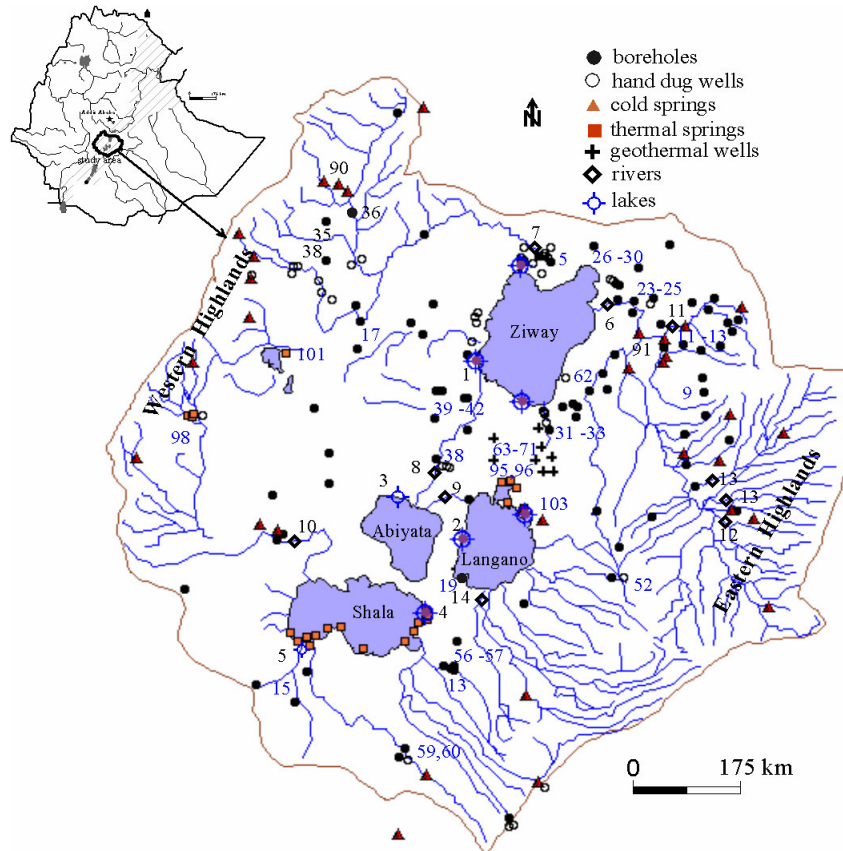


Figure 1. Location map (including sampling sites).

et al., 1987; Darling et al., 1996; Gizaw, 1996; Chernet et al., 2001). Very few studies provided information on how groundwater quality is influenced along flow paths at regional scale all the way from the Ethiopian highlands to the rift (Ayenew, 2005; Kebede et al., 2005). Some studies revealed temporal changes of the quality of the lakes caused by anthropogenic influences (Ayenew and Legesse, 2007).

Water well drilling programs have been initiated over the last few decades, but groundwater provision is often unsuccessful because of poor water quality and productivity. This problem is exacerbated by lack of understanding of the groundwater flow system. Information on groundwater circulation and hydrochemical evolution is poorly understood, except few general studies made at sub-regional scale (Chernet et al., 2001; Ayenew, 2003). Groundwater circulation patterns, recharge source and interactions between lakes and groundwaters have also been the subject of few studies in the southern MER (McKenzie et al., 2001). These studies indicate rift-ward groundwater flow from adjacent highlands. However little is known about the detailed hydrochemistry and geochemical evolution, which has practical implication for well drilling site selection and sustainable use of the groundwater resources.

In this study, attempt is made to understand the spatial

variation of hydrochemical facies and the underlying causes in relation to the movement and occurrence of groundwater. Special emphasis is given to the geochemical evolution across the rift accounting the different volcanic rock sequences and geomorphological zones.

General description of the basin

The ZSB is located in central Ethiopia bounded within the limits of 38° 00'-39° 30' east longitude and 7° 00'-8° 30' north latitude, and covers a total area of 13,000 km² (Figure 1). The central part is the floor of the rift occupied by lakes Ziway, Langano, Abiyata and Shala with distinct hydrogeological and hydrochemical setting (Table 1). The basin can be divided into three geomorphological zones: the rift floor, the transitional escarpments and the highlands. The altitude ranges from over 2900 meters above sea level (m.a.s.l) in most parts of the surface water divide in the highlands to 1600 m.a.s.l. around the lakes. The basin has a closed surface water drainage system. The water divide is characterized by elongated volcanic ridges to the east and west and in other places by isolated volcanic hills. The lakes are believed to have been formed by volcano-tectonic processes (Street, 1979). Shala and Abiyata are alkaline terminal lakes with no surface water outlets. There are many geothermal manifestations

Table 1. Basic morphometric and hydrochemical data of the lakes (ionic concentrations are in meq/l and EC in $\mu\text{S/cm}$). Note. The morphometric data is for the late 1990s. The size and level of Ziway and Abiyata have been reduced significantly in recent years.

Lakes	Altitude (m.asl)	Area (km ²)	Maximum depth(m)	Mean depth (m)	Catchment area (km ²)	pH	Ca	Mg	Na	K	CO ₃	CO ₃	HCO ₃ ³⁻	HCO ₃	Cl	SO ₄	F	EC
Abiyata	1580	180	14.2	7.6	10740	9.9	3.2	2.1	5387.6	257	2.8	625.5	85.6	522.9	1611.8	494.7	19	19484
Langanjo	1585	230	47.9	17	2000	9.2	4.8	2.6	445.1	24.1	1.4	313.3	7.2	436.4	113.5	29.6	13.6	1736.7
Shala	1550	370	266	86	2300	9.8	3.6	3.7	6344.6	257.6	157.1	4714.7	88.3	5385.4	217.1	244.1	155.2	21545
Ziway	1636	440	8.9	2.5	7380	9.4	5.6	3.4	2474.9	112.6	74.9	2242.2	36.8	2244.7	772.7	155.6	72.3	192.3

(fumaroles, hot springs, hot wells) in the rift.

The climate is humid to sub-humid in the highlands and semi-arid in the rift floor. The mean annual rainfall is about 600 mm in the vicinity of lake Ziway, and rises to a maximum of 1200 mm in the highlands. Mean annual temperature varies between 15°C in the highlands and 20°C in the lowlands.

Geologically the basin has complex history. The central sector and the shoulders of the MER are made of vulcanites and pyroclastic rocks, whereas large areas of the rift floor are covered with volcano-lacustrine and fluvio-lacustrine deposits underlain by thick ignimbrites (Merla et al., 1979). The oldest volcanic rocks (Plateau Trap Series) are exposed in the western escarpment and consist of basaltic lava flows, with inter-bedded ignimbritic beds, overlain by massive rhyolites, tuffs and basalts. Miocene to Pliocene basalt flows; rhyolites and tuffs unconformably cap the Early Tertiary volcanic units (Woldegabriel et al., 1990). The eastern plateau is covered with Pliocene to Early Pleistocene shield volcanoes consisting of trachytes and basalts, with mugearites and phonolites (Di Paola, 1972).

Silicic pyroclastic materials cover the escarpments and the rift floor. They are mainly peralkaline rhyolitic ignimbrites, interlayered with basalts and tuffs and associated pumices. Alkaline and peralkaline rhyolitic lava flows and domes, asso-

ciated with pumice and ash represent the late silicic volcanic events in the basin (Di Paola, 1972). These lavas were erupted from remnants of large calderas. A more recent volcanic unit, crops out along the tectonically active Silte - Debrezeit Fault Zone (SDFZ) and the Wonji Fault Belt (WFB); it is made up of basaltic lava flows associated with hyaloclastites and scoria cones. Young volcanoes and calderas, such as the Bora - Bericcio complex, the Aluto volcano and the Corbetti calderas are made up of rhyolitic lava flows, unwelded pumice falls and ashes. Obsidian flows represent the final product of the volcanic activity (Mohr, 1983). Late Quaternary fluvio-lacustrine sediments cover large area of the rift. They were laid down in a very wide single lake. The four present-day lakes are the remnants of that ancient lake (Street, 1979).

The focal area in this study is confined in a NNE trending structure formed by a line of young faults and volcanic centres in the rift floor close to the eastern escarpment, and arranged in an échelon fashion. This volcano-tectonic axis, named the WFB, is considered to be the current axis of crustal extension. Faults along this active zone form numerous minor horsts and grabens or "rift-in-rift" structures. The western escarpment is primarily characterized by one major fault scarp. It shows a high throw in its north-eastern part, which progressively decreases and dies out to the south-

west where it has been covered by volcanic products. However, in the western escarpment along the Guraghe Mountains, more than 1.5 km thick flood basalt is displaced by several step faults that strike NNE. These faults are cut by northwest and west striking transverse fault

The permeability of the rocks is highly variable based on the degree of weathering and faulting. The hydraulic conductivity varies in a wide range between 0.1 and 140 m/d, the highest being in the rift floor. Groundwater moves from all sides towards the centre of the basin into the lakes. The rift floor groundwater movement is strongly controlled by the axial faults. This has been illustrated by isotopic studies and groundwater models (Ayenew, 2001; 2003). Much of the water-bearing zones in the highlands are within the weathered volcanic sequence and locally in inter-bedded river gravels and alluvial deposits. The majority of faults are conduits to groundwater flow. In places these open faults allow significant amount of preferential groundwater flow parallel and sub-parallel to the rift axis. In the rift floor the direction of groundwater is strongly controlled by the orientation of faults, which is often perpendicular to the regional groundwater contours in the highlands and escarpments. The axial faults control the subsurface hydraulic connection of the rift lakes and the river-groundwater relations (Ayenew, 2005).

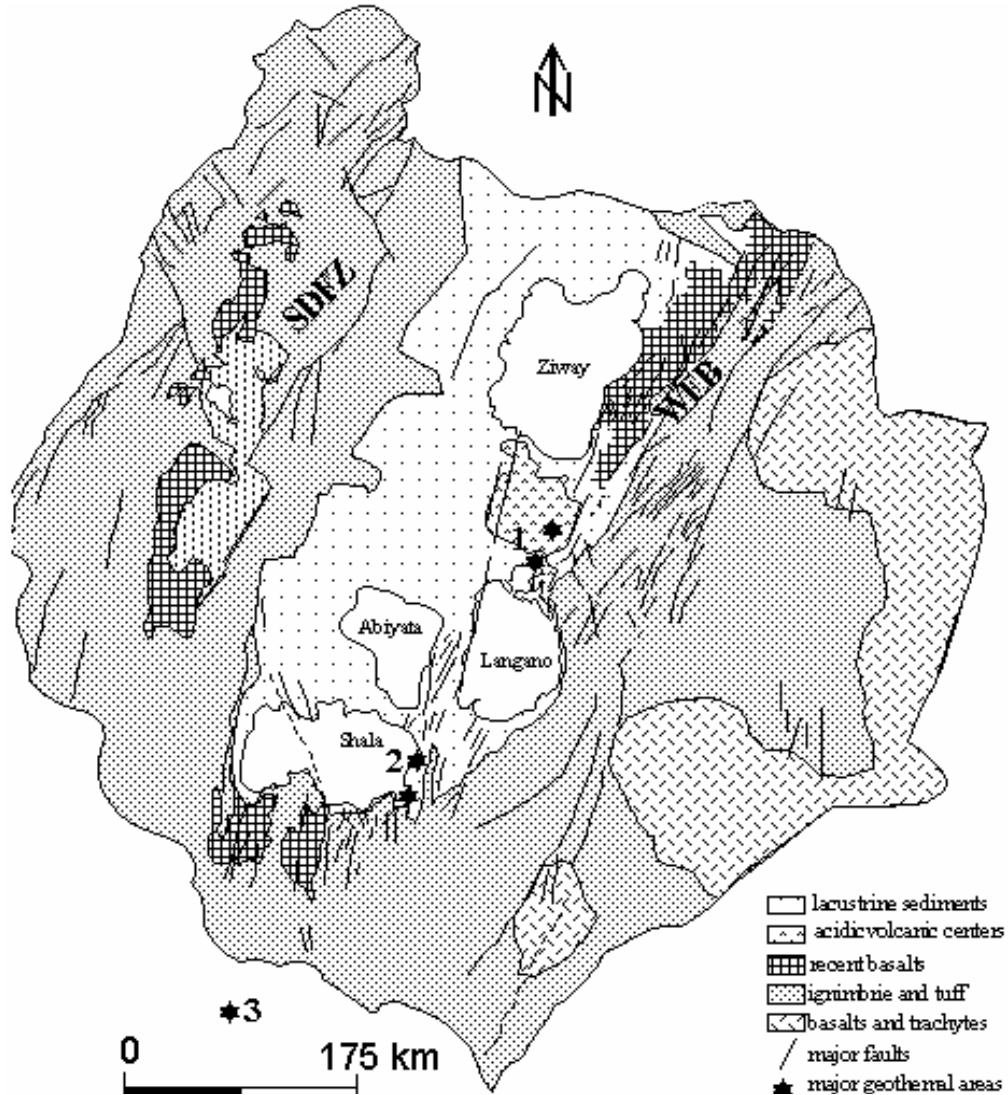


Figure 2. Simplified hydrogeological map of ZSB (numbers indicate major geothermal centers: 1 = Aluto - Langano; 2 = Shala, 3 = Corbetti).

Approach and methodology

Before water sampling, extensive field hydrogeological mapping was carried out to develop the preliminary conceptual hydrogeological view of the basin (Figure 2). This helped to identify sampling points for systematic hydrogeochemical and cluster analysis. In addition to the newly generated hydrochemical data, existing data are used as supplementary information. The sampling sites were chosen carefully based on sound hydrogeological reasoning pertinent to the occurrence and movement of groundwater and localization of surface water bodies.

A total of 126 water samples were collected from wells, springs, lakes and rivers (Table 2). The samples were kept in polyethylene sample bottles and completely filled and tightened with plastic caps. Electrical conductivity (EC), pH and temperature were measured in the field.

Lake water samples were collected from the top few centimeters of the surface and at a distance of about five to ten meters from the shores. Spring samples were collected from the point of emanation using new plastic syringes. A special stainless steel groundwater sampling apparatus was used for boreholes and hand dug wells.

Major cations (Ca, Mg, Na and K) were measured by Atomic Absorption Spectrophotometry and some anions (Cl, SO₄ and F) by Ion Chromatography. Carbonate and bicarbonate were determined by titration. As the samples were analyzed in different laboratories and collected from various sources the analytical errors are variable. For the majority of the samples the analytical error is less than 4.5%. For the great majority of the data error is less than 2%. From the point of view of showing the spatial variations at the mapping scale (1:250,000) the quality of the data is believed to be satisfactory.

Table 2. Chemical analysis result of ions for selected water samples (meq/l) and saturation indices calculated by PHREEQC-2 (Note: BH = Borehole, TW = thermal well, DW = dug well, CS = cold spring, HS = hot spring: Values with zero indicate trace or not determined). For some samples pH and EC were not determined. The GPS locations for some samples is not known exactly.

No.	ID	Sample ID	Type	X	Y	Ca	Mg	Na	K	CO ₃	HCO ₃	Cl	SO ₄	TDS	F	pH	Cond	SI_Calcite	SI_Fluorite
1	10	BH-10	Gw	484614	857721	0.09	0.02	44.15	3.53	0.00	26.99	18.93	1.36	3991	1.46	8.40	3350	0.1094	-0.025
2	11	BH-11	Gw	484888	854858	0.07	0.04	31.54	1.23	0.00	9.90	17.24	1.67	2433	1.21	9.52	2990	0.4467	-0.3222
3	12	BH-12	Gw	482908	854827	0.06	0.02	37.15	1.20	0.00	28.99	8.52	0.32	3349	1.42	8.24	2880	-0.1913	-0.2195
4	13	BH-13	Gw	481995	863631	0.02	0.01	35.67	3.20	0.00	23.99	11.34	0.91	3192	2.53	7.38	2750	-1.5467	-0.1441
5	14	BH-14	HS	474644	852428	0.07	0.04	38.06	1.18	0.00	25.99	9.65	0.20	3091	2.69			-1.2838	0.5154
6	15	BH-15	HS	442949	822948	0.02	0.04	56.55	2.05	0.00	38.99	13.71	0.67	4424	1.53			-1.7866	-0.6711
7	16	BH-16	DW	464706	855772	0.05	0.04	33.06	0.51	0.60	23.93	4.51	2.29	2800	1.95			-1.6169	-0.0556
8	17	BH-17	TW	481477	857142	0.01	0.01	26.93	3.91	0.00	16.49	7.14	3.19	2977	2.15	6.70	2110	-2.3582	-0.2467
9	18	BH-18	TW			0.02	0.02	28.84	0.77	0.00	21.57	0.76	2.44	2396	2.42	9.17	2010	-0.1123	-0.3764
10	19	BH-19	TW	480927	855133	0.05	0.02	24.49	1.28	0.00	36.96	1.44	2.74	3354	1.37	10.26	2300	0.4683	-1.0796
11	20	BH-20	TW			0.05	0.01	28.84	1.02	0.00	16.49	0.62	4.62	2297	0.95	9.71	2120	0.3089	-1.0016
12	21	BH-21	TW	481672	854871	0.05	0.01	36.97	1.28	0.00	25.30	0.56	3.20	3067	3.53	8.69	2640	-0.0734	0.3271
13	22	BH-22	BH	412288	830368	1.00	0.33	3.48	0.31	0.20	6.00	0.31	0.01	637	0.16			-0.5792	-0.5455
14	23	BH-23	BH	429285	849711	0.55	0.49	1.91	0.23	0.00	4.13	0.11	0.02	871	0.07			-0.972	-1.4906
15	24	BH-24	BH	437765	867465	1.27	0.37	6.96	0.43	0.00	9.34	0.82	0.27	963	0.15			-0.3382	-0.5642
16	25	BH-25	BH	480305	901414	1.37	0.29	1.48	0.08	0.00	4.65	0.17	0.08	473				-0.5262	
17	26	BH-26	BH	480599	901616	1.15	0.25	3.18	0.10	0.00	5.82	0.39	0.03	579	0.07			-0.5318	-1.2009
18	27	BH-27	BH	521251	846143	0.84	0.42	0.96	0.09	0.00	3.32	0.10	0.00	230	0.01			-0.8586	-2.9684
19	28	BH-28	BH	512683	851346	0.54	0.36	0.65	0.11	0.00	2.20	0.15	0.00	180	0.06			-1.2046	-1.5739
20	30	BH-30	BH	511000	856242	1.12	0.49	1.04	0.13	0.00	4.16	0.20	0.00	285	0.08			-0.6543	-1.0601
21	31	BH-31	BH	516644	889724	1.15	0.36	0.94	0.15	0.00	3.80	0.20	0.00	326				-0.6786	
22	32	BH-32	BH	507899	900677	1.55	0.08	13.57	0.51	0.00	16.60	0.37	0.00	1155				-0.0711	
23	33	BH-33	BH	497565	889283	0.57	0.45	2.04	0.24	0.00	4.00	0.20	0.00	360				-0.9537	
24	34	BH-34	BH	486788	867554	0.70	0.40	3.04	0.13	0.00	4.80	0.39	0.00	398				-0.8105	
25	35	BH-35	BH	465405	810049	0.60	0.51	3.20	0.65	0.00	3.00	0.71	0.01	1137	0.03	6.94	2030	-1.13	-2.1888
26	36	BH-36	BH	519294	884778	1.15	0.36	0.94	0.15	0.00	3.80	0.20	0.00	326	0.06			-0.6792	-1.2923
27	37	BH-37	BH	504694	889596	0.72	0.68	2.77	0.37	0.00	4.40	0.05	0.01	210	0.08	7.60	347	-0.2395	-1.2736
28	38	BH-38	CS	426704	843799	0.52	0.70	3.18	0.26	0.00	5.21	0.25	0.22	140	0.14			-0.9187	-0.9447
29	39	BH-39	CS	506276	876854	1.15	0.21	1.48	0.14	0.00	1.40	0.20	0.04	72	0.15	7.65	121	-0.4407	-0.4646
30	40	BH-40	CS	424762	885865	0.72	0.37	0.43	0.13	0.00	1.46	0.08	0.06	185	0.02			-1.2503	-2.395
31	41	BH-41	CS	422821	902692	1.02	0.53	1.00	0.31	0.00	2.21	0.08	0.05	290	0.02			-0.947	-2.2802
32	42	BH-42	CS	439648	913371	0.45	0.45	0.17	0.13	0.00	1.39	0.14	0.03	267	0.02			-1.4758	-2.599
33	43	BH-43	DW	445221	896905	0.90	0.62	1.96	0.26	0.00	5.00	0.23	0.14	524	0.01			-0.6888	-2.9862
34	44	BH-44	DW	441433	889599	1.15	0.37	6.31	0.43	0.00	9.06	0.39	0.10	885	0.14			-0.3894	-0.66
35	45	BH-45	DW	482837	895011	1.07	0.33	7.18	0.51	0.00	8.51	0.45	0.24	867	0.10			-0.4422	-0.9776
36	46	BH-46	DW	483254	898446	0.97	0.21	1.61	0.18	0.00	3.65	0.31	0.21	1030	0.05			-0.7686	-1.5202
37	47	BH-47	DW	483519	899062	1.12	0.41	7.83	0.46	0.00	10.26	1.35	0.19	1030	0.26			-0.3652	-0.1569
38	48	BH-48	DW	480943	897176	1.72	0.12	1.22	0.13	0.00	4.92	0.23	0.02	493	0.04			-0.4091	-1.4857
39	49	BH-49	DW	469720	885980	1.40	1.00	6.96	0.29	0.00	11.00	4.00	0.55	596	0.80	7.54	990	0.2681	0.8723
40	52	BH-52	DW	415724	866326	0.77	0.49	0.52	0.15	0.00	3.10	0.23	0.06	330	0.02			-0.9182	-2.397
41	53	BH-53	DW	441231	891781	1.25	0.86	6.52	0.59	0.00	10.29	0.31	0.09	987	0.22	0.0		-0.3139	-0.2573
42	54	BH-54	DW	433855	896364	1.52	0.58	1.65	0.31	0.00	5.47	0.65	0.07	574	0.00			-0.4339	
43	56	BH-56	DW	434667	896364	1.40	0.74	1.87	0.36	0.00	6.00	0.20	0.19	636	0.01			-0.4369	-2.8186
44	57	BH-57	BH	510649	869224	1.10	0.86	0.85	0.16	0.68	2.74	0.20	0.26	330	0.08			-0.8404	-1.0712
45	58	BH-58	BH	445942	888136	1.80	0.50	1.48	0.15	0.50	4.80	0.07	0.02	362	0.08	7.07	599	-0.337	-0.879
46	6	BH-6	CS	476206	852307	0.80	0.40	3.26	0.57	0.97	2.33	1.00	0.14	327	0.12	7.35	654	-0.7073	-0.8589
47	62	BH-62	CS	478784	846641	0.92	0.40	1.20	0.30	0.73	2.03	0.80	0.00	155	0.10	6.72	310	-1.3077	-0.9243

Table 2 Contd.

No.	ID	Sample ID	Type	X	Y	Ca	Mg	Na	K	CO ₃	HCO ₃	Cl	SO ₄	TDS	F	pH	Cond SI	Calcite SI	Fluorite
48	64	BH-64	HS	476071	852375	0.96	0.80	5.00	0.90	0.73	2.62	3.62	0.44	330	0.10	6.92	660	-1.0514	-0.9994
49	65	BH-65	HS	469455	850822	1.16	0.45	6.00	1.20	0.50	4.10	3.41	0.44	315	0.11	6.71	630	-1.0004	-0.8475
50	67	BH-67	HS	476776	849776	1.88	0.66	23.00	1.30	0.50	18.45	9.00	0.05	1649	1.20	6.59	3298	-0.4125	1.2486
51	7	BH-7	DW	439538	890952	1.15	1.87	9.79	0.26	0.25	12.50	1.35	0.48	1347	0.15			-0.3091	-0.6915
52	79	BH-79	BH	440615	832269	0.02	0.04	15.44	2.56	2.30	9.29	0.96	0.12	1374	3.95			-2.1904	0.4208
53	8	BH-8	BH	466726	839869	0.01	0.02	19.97	0.74	1.50	10.00	8.01	0.04	1602	0.68	0.0		-2.1736	-1.1287
54	80	BH-80	BH	467649	866929	0.10	0.07	10.87	0.30	1.61	7.60	0.40	0.00	899	0.10	7.5		-1.0199	-2.0009
55	81	BH-81	BH	456844	884690	0.05	0.04	11.53	2.03	0.00	10.24	0.28	0.12	988	0.79			-1.8188	-0.6408
56	82	BH-82	BH	467974	863049	0.35	0.21	9.57	1.68	0.00	9.83	0.59	0.08	894	0.32			-0.8966	-0.4859
57	84	BH-84	BH	470161	868877	0.22	0.08	10.47	1.84	0.00	10.11	0.00	0.56	600	0.10	8.30	1200	0.1708	-1.7276
58	87	BH-87	DW	469472	871897	0.24	0.04	17.74	3.12	0.00	17.68	0.06	0.00	70	0.28	8.61	110	0.6236	-0.9307
59	9	BH-9	DW	468340	885071	0.34	0.04	13.26	2.33	0.00	13.12	0.28	0.00	96	0.24	8.33	150	0.4696	-0.8149
60	91	BH-91	BH	430345	840524	0.05	0.04	11.74	0.41	0.00	10.98	0.24	0.10	1112	0.63			-1.7871	-0.835
61	339	BH-96	BH	440503	858367	0.15	0.08	9.13	0.38	0.00	8.67	1.02	0.30	871	0.44			-1.3258	-0.5793
62	340	BH-97	BH	446686	885043	0.47	0.21	6.09	0.41	0.00	6.85	0.45	0.06	776	0.14			-0.8574	-0.9988
63	104	CS-11	BH	467797	878153	0.35	0.37	8.70	0.38	0.20	7.75	0.51	0.05	934	0.17			-0.9748	-1.0087
64	105	CS-12	BH	480403	900580	0.35	0.37	8.70	0.38	0.20	9.39	0.51	0.05	934	0.17			-0.9043	-1.0232
65	106	CS-13	BH	459810	832677	0.07	0.02	13.62	0.64	0.40	7.60	6.01	0.03	1175	0.40			-1.6483	-0.9351
66	107	CS-14	BH	462304	867052	0.06	0.02	5.17	0.91	0.00	4.92	0.00	0.24	220	0.10	8.80	440	-0.1706	-2.218
67	112	CS-19	BH	455519	798303	0.40	0.33	8.48	0.46	0.30	9.00	0.42	0.07	915	0.17			-0.8486	-0.9476
68	114	CS-21	BH	467183	869410	0.72	0.68	10.00	0.37	0.50	11.50	0.05	0.01	572	0.08	8.44	953	0.8585	-1.4302
69	115	CS-22	BH	426105	811287	0.15	0.08	8.70	0.31	0.10	6.70	1.21	0.48	843	0.58			-1.4265	-0.3261
70	116	CS-23	BH	491948	870967	0.57	0.58	6.79	0.25	0.30	10.50	0.13	0.08	552	0.15	8.17	924	0.5085	-0.9292
71	120	CS-27	DW	460633	853379	0.72	0.25	5.65	0.31	0.00	7.54	0.65	0.07	750	0.24			-0.6483	-0.365
72	96	CS-3	DW	470118	886893	0.52	0.33	19.84	0.51	0.00	16.32	3.64	0.77	1806	0.11			-0.5831	-1.3398
73	126	CS-33	DW	484157	898238	0.57	0.21	6.96	0.36	0.00	8.51	0.82	0.01	829	0.08			-0.7006	-1.4258
74	127	CS-34	DW	487438	873903	0.90	0.58	15.01	0.84	0.00	16.50	1.35	0.34	1571	0.53			-0.3216	0.2841
75	341	CS-38	DW	479108	901415	0.57	0.21	6.96	0.36	0.00	8.46	0.82	0.01	829	0.08	7.8		0.0851	-1.4336
76	342	CS-39	Gw	473069	857081	0.02	0.01	24.19	0.97	0.00	16.32	6.52	0.26	1969	1.32	9.34	1860	-0.0753	-0.8717
77	97	CS-4	Gw	473130	861620	0.02	0.01	3.87	0.51	0.00	3.38	0.59	0.06	401	0.11	9.40	350	-0.3369	-2.6481
78	98	CS-5	HS	432095	878479	0.20	0.08	9.79	0.59	0.00	9.83	0.62	0.02	1032	0.27		3000	-1.1198	-0.8533
79	99	CS-6	BH	431494	841849	0.42	0.10	4.35	0.77	0.00	5.74	0.10	0.07	612	0.21			-0.9713	-0.6775
80	101	CS-8	BH	461289	816541	0.35	0.16	0.87	0.10	0.00	1.64	0.06	0.24	265	0.05			-1.5274	-1.9215
81	102	CS-9	BH	464529	814467	0.35	0.16	1.09	0.08	0.00	2.29	0.07	0.08	287	0.05			-1.3874	-1.9279
82	139	DW-10	BH			0.27	0.12	0.52	0.10	0.00	1.34	0.00	0.08	203	0.02			-1.6775	-2.7754
83	140	DW-11	BH	465118	815630	0.42	0.12	0.65	0.10	0.00	1.47	0.16	0.11	219	0.03			-1.4737	-2.2619
84	141	DW-12	BH	514701	870557	0.32	0.10	0.78	0.05	0.00	1.50	0.20	0.00	125	0.02			-1.5754	-2.7233
85	142	DW-13	BH	514259	873560	0.40	0.09	0.47	0.05	0.00	1.30	0.20	0.00	167	0.01			-1.5348	-3.2215
86	143	DW-14	BH	501805	895996	0.42	0.16	1.53	0.21	0.00	3.50	0.19	0.00	312				-1.1329	
87	144	DW-15	BH			0.37	0.25	1.57	0.16	0.00	2.70	0.19	0.00	264				-1.3024	
88	146	DW-17	BH			0.75	0.13	3.24	0.57	0.00	2.30	1.75	0.01	108	0.06	7.55	216	-0.5436	-1.4856
89	147	DW-18	BH	498006	892374	0.38	0.14	2.71	0.31	0.00	3.70	0.19	0.00	288				-1.1646	
90	148	DW-19	BH	469716	890725	0.76	0.18	1.49	0.26	0.00	2.16	0.00	0.15	205	0.12	7.89	410	-0.1979	-0.8414
91	149	DW-20	BH	461694	809225	0.23	0.19	1.77	0.31	0.00	2.10	0.00	0.02	116	0.07	7.65	232	-0.9693	-1.8291
92	150	DW-21	BH	466281	808649	0.40	0.20	2.97	0.52	0.00	3.54	0.00	0.03	123		7.72	246	-0.4509	
93	151	DW-22	BH			0.28	0.25	1.61	0.28	0.00	1.80	0.28	0.04	128	0.02	6.30	255	-2.2761	-2.8116
94	152	DW-23	BH	500000	883000	0.49	0.22	1.00	0.09	0.00	2.02	0.05	0.01	122	0.06	7.52	190	-0.7706	-1.6177
95	153	DW-24	BH	461137	815099	0.29	0.26	3.00	0.30	0.00	1.68	0.51	0.01	616	0.02	7.36	1100	-1.2623	-2.8298
96	154	DW-25	BH			0.33	0.27	2.90	0.60	0.00	3.00	0.54	0.04	582	0.02	6.55	1040	-1.7803	-2.7941

Table 2 Contd.

No.	Sample			X	Y	Ca	Mg	Na	K	CO3	HCO3	Cl	SO4	TDS	F	pH	Cond	SI_Calcite	SI_Fluorite
	ID	ID	Type																
97	165	DW-36	BH			0.32	0.16	1.70	0.30	0.00	1.56	0.56	0.02	150	0.03	7.52	300	-1.0624	-2.3995
98	166	DW-37	BH	472794	814100	0.35	0.30	2.80	0.12	0.00	1.80	0.54	0.01	381	0.00	7.18	680	-1.3274	
99	133	DW-4	BH	465424	810049	0.80	0.30	2.00	0.50	0.00	4.00	0.17	0.01	81	0.05	8.00	162	0.168	-1.6192
100	134	DW-5	BH			0.56	0.09	1.84	0.32	0.00	1.52	0.90	0.04	98	0.03	6.46	196	-1.8963	-2.1648
101	182	DW-53	BH	489060	838182	0.45	0.23	1.39	0.25	0.00	2.06	0.00	0.01	121		7.45	242	-0.8746	
102	135	DW-6	BH	454459	796536	0.25	0.08	0.61	0.13	0.00	0.88	0.20	0.04	160	0.04			-1.9183	-2.2296
103	343	DW-60	BH	465705	820049	0.20	0.10	1.20	0.40	0.00	1.80	0.06	0.02	114	0.08	8.06	183	-0.6629	-1.7419
104	344	DW-61	BH	495517	871107	0.29	0.21	3.47	0.29	0.10	2.80	0.51	0.17	155	0.09	7.85	255	-0.5802	-1.5526
105	136	DW-7	BH	497428	892538	0.00	0.00	3.36	0.36	0.50	3.70	0.13	0.03	219	0.11	7.92	362		
106	137	DW-8	CS	444178	911429	0.45	0.29	0.65	0.15	0.00	2.43	0.14	0.03	563	0.02			-1.2512	-2.6162
107	189	GTW-1	CS	530538	862393	0.14	0.08	0.13	0.03	0.00	0.51	0.02	0.03	70	0.01			-2.3616	-3.6345
108	190	GTW-2	CS	479449	809174	0.22	0.08	0.43	0.18	0.00	1.00	0.08	0.09	179	0.01			-1.9015	-3.472
109	191	GTW-3	CS	457659	794355	0.15	0.12	0.48	0.10	0.00	0.70	0.51	0.02	164	0.11			-2.2485	-1.5821
110	192	GTW-4	CS	476408	851396	0.36	0.10	1.40	1.00	0.73	1.77	0.40	0.03	139	0.09	6.80	272	-1.6803	-1.3997
111	193	GTW-5	CS	470839	851126	0.32	0.11	2.00	0.90	0.73	1.57	0.45	0.03	138	0.09	6.77	276	-1.8156	-1.4543
112	195	GTW-7	CS	479186	846962	0.24	0.14	1.48	0.15	0.30	2.70	0.07	0.02	161	0.08	7.25	269	-1.224	-1.6782
113	196	GTW-8	CS	506994	877916	0.21	0.16	0.46	0.08	0.00	1.30	0.02	0.00	73	0.02	7.60	119	-1.232	-2.9147
114	206	HS-10	CS	521768	832489	0.25	0.13	0.22	0.02	0.00	0.90	0.08	0.03	106	0.01	6.7		-2.199	-3.4234
115	222	HS-26	CS	511928	879536	0.35	0.21	0.35	0.08	0.00	1.46	0.08	0.06	185	0.02	0.0		-1.5596	-2.6972
116	113	Hs-27	CS	413760	876805	0.32	0.29	1.04	0.13	0.00	2.43	0.23	0.06	311	0.03			-1.3927	-2.4061
117	117	Hs-28	CS	424762	893632	0.45	0.21	0.87	0.23	0.00	2.39	0.06	0.03	254	0.02			-1.2584	-2.6146
118	118	Hs-29	DW	475005	784673	0.25	0.16	0.43	0.51	0.00	1.02	0.51	0.07	164	0.01			-1.8682	-3.452
119	202	HS-6	DW	475010	784660	0.25	0.12	0.22	0.03	0.00	0.56	0.45	0.01	100	0.00			-2.1031	
120	203	HS-7	DW	496368	893658	0.57	0.16	2.17	0.15	0.00	3.88	0.11	0.03	407	0.14			-0.963	-0.8452
121	204	HS-8	DW	456317	796236	0.27	0.25	1.48	0.56	0.00	2.98	0.11	0.01	366	0.03			-1.3738	-2.4774
122	323	TW-1	DW	415724	866326	0.25	0.25	0.78	0.38	0.00	1.79	0.17	0.01	266	0.03			-1.635	-2.5124
123	324	TW-2	HS	478784	846641	0.29	0.21	3.47	0.29	0.50	5.10	0.51	0.17	367	0.09	7.46	587	-0.7307	-1.5799
124	325	TW-3	TW			0.40	0.12	2.39	0.20	0.00	3.74	0.17	0.01	423	0.09	7.7		-0.4422	-1.3881
125	326	TW-4	HS	412731	865888	0.40	0.12	2.39	0.20	0.00	3.74	0.17	0.01	423	0.09			-1.1362	-1.3848
126	345	TW-5	BH	435998	813937	0.09	0.02	45.67	1.94	0.70	30.99	11.23	0.48	4100	2.37			-1.2421	0.363

The hydrochemical data have been used to categorize the waters in to different objective water classes on the basis of Q-mode statistical cluster analysis. Statistical classification of geochemical data by Q-mode hierarchical cluster analysis (HCA) has been proven to provide a suitable basis for objective classification of water composition into hydrochemical facies (Meng and Maynard, 2001; Güler et al., 2002, Güler and Thyne 2003; Kebede et al., 2005). HCA is a multivariate statistical technique intended to classify hydrochemical observations so that the members of the resulting groups or subgroups are similar to each other and distinct from the other groups. The characteristics of the groups or sub-groups are not predetermined but can be obtained after the classification. The results obtained in HCA are justified according to their values in interpreting the data and in indicating realistic hydrochemical patterns representing field conditions. It is therefore not the number of members of a

group that determines the robustness of HCA. It is possible that many single member groups that do not belong to any of the multi-member groups are placed in separate groups. This classification is useful especially to understand geological controls on water chemistry under conditions where useful geochemical data are available but clear hydrogeologic models have not yet been developed. The advantage of HCA is that many variables can be used to classify waters. In order that the variables have equal weight the raw chemical data have been log-transformed and standardized. This restricts the influence of or the biases caused by the variables that have the greatest or the smallest variances or magnitudes on the clustering result. A detailed description of the advantages and uses of the HCA in hydrochemistry and the mathematical formulation behind HCA is thoroughly discussed in Güler et al. (2002).

The ability of HCA to classify groundwater chemistry

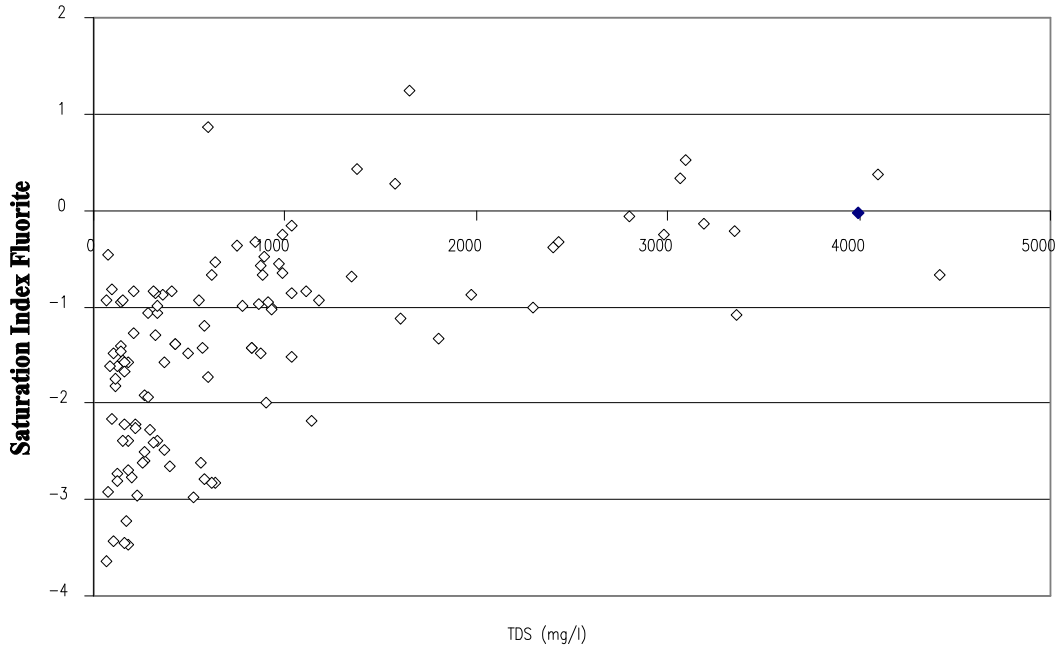


Figure 4. Scatter plots of hydrochemical variables pertinent to the assessment of the groundwater hydrochemical evolution and dynamics (concentration in meq/l).

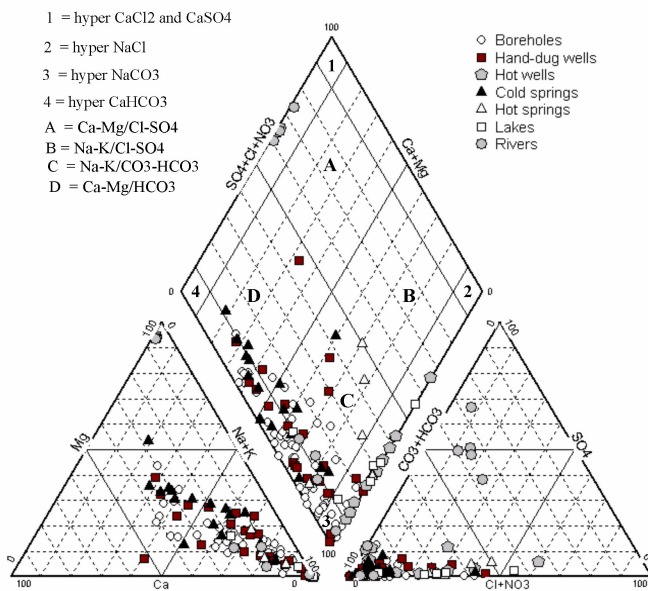


Figure 3. Piper plots of water samples (concentration in meq/l).

into coherent groups that may be distinguished in terms of aquifer type, subsurface residence time and degree of human impact on water chemistry provides a good opportunity to conduct hydrogeochemical modeling and understand groundwater geochemical evolution among the different groups or subgroups. In this study, HCA is used to classify waters into objective groups. A Microsoft-Excel® add-in module XLSTAT 4.3 was used to conduct

the HCA.

The same hydrochemical data set was used in the hydrogeochemical modeling software called PHREEQC-2 (Parkhurst and Appelo, 1999). In this study PHREEQC-2 is used for geochemical calculations of saturation indices.

RESULTS

Table 2 summarizes the hydrochemical analysis result and saturation indices calculated by PHREEQC-2. Figures 3 and 4 are Piper and scatter diagrams showing the relations of different hydrochemical variables which have relevance to the hydrochemical evolution and groundwater flow dynamics.

The hydrochemical analysis and field measured water quality variables (EC, pH) shows wide hydrochemical variations. In general sodium and bicarbonate represent the dominant cation and anion, respectively. The majority of the groundwater samples have sodium concentration ranging from 60 to 300 mg/l; while for bicarbonate it ranges from 200 to 600 mg/l. The variability in cation concentration is more pronounced than the anions. The dominance of bicarbonate over other anions has been explained in terms of reactions of dissolved carbon-dioxide and the influence of geothermal systems (Gizaw, 1996). In thermal waters HCO_3 is the most important anion. Fournier and Truesdell (1970) suggested that in geo-thermal systems most of the HCO_3 and part of the Na and K are produced by the reaction of dissolved CO_2 . Surface geochemical survey of the rift waters in Langanjo and Aluto areas suggested similar mechanism of HCO_3 enrichment

(UNDP, 1973). Potassium, the second dominant cation in the thermal waters of the area, shows a tendency to increase with temperature, reaching up to about 200 mg/l at 360 °C.

The dominance of Na and HCO₃ is clearly evident from the Piper diagram (Figure 3). It displays at least three groups of waters representing the three physiographic regions. These are Ca-Mg-HCO₃, Na-HCO₃ and mixed types (between the two end members) representing the highlands, rift and escarpments, respectively. This indicates the existence of different hydrochemical facies, which corresponds to different types of flow regimen across the rift valley. Local, intermediate and regional flow systems have been identified across the rift from conventional hydrogeological studies and groundwater flow modeling (Ayenew, 1998; 2001). The majority of the waters are dominantly Na-HCO₃ followed by Ca-Mg-HCO₃ type. There are also distinct differences in total ionic concentration, alkalinity and cation species across the rift. These differences are related to variations in lithology, groundwater recharge rates, temperature gradients and residence time of groundwater.

The majority of the cold springs, hand dug wells and boreholes in the highlands are Ca-Mg-HCO₃ type waters, which tend to be Na-Ca-HCO₃ types in the transitional escarpments. Due to high groundwater recharge from rainfall and low groundwater residence time the TDS is mostly less than 250 mg/l in the highlands. The high Ca and Mg content in the highlands are related to the dominance of the basic volcanics (basalt) in clear contrast with the rift floor acidic volcanics such as ignimbrite, tuff and pumice. As revealed from geochemical groundwater evolution analysis in different parts of the world, the Ca-Mg-HCO₃ type waters are often regarded as recharge area waters at their early stage of geochemical evolution (Plummer et al., 1990; Adams et al., 2001; Edmunds and Smedley, 2000). They are rapidly circulating ground waters, which have not undergone a pronounced rock-water interaction.

A preliminary study of the TDS and major ions relationships showed that in most dilute waters, calcium content is increasing up to 3.7 meq/l, and then decreases regularly. This change could be attributed to calcite precipitation (Chernet et al., 2001). The sodium enrichment seems to be rather uniform and could correspond to dilution or concentration of a unique salinity source (silicate hydrolysis). Chloride and sulfate mainly follows an evaporative pattern, but are locally enhanced in the rift. This evolution may reflect a distinct secondary salinity source, which involves salt supplies of different origins. The secondary salinity sources are likely to be related to the rift floor sediments, mainly lacustrine deposits.

In general the total ionic enrichment follows the groundwater flow path from the highlands to the rift floor. The ionic composition of the water samples indicates relatively variable chemical facies; waters are Ca, Mg, and HCO₃-dominated for the diluted waters, and become Na

and HCO₃ dominated with steady increase of Chloride (Cl) in most concentrated waters. A small group of samples provide mixed facies with higher SO₄. This change may be attributed to local mixing with the deep thermal waters of the rift.

The only exception in the highlands is the hydrochemical signature of the low-temperature hot springs (103 and 104) located in the western escarpment. They are Na-HCO₃ type waters, which have more or less similar composition as some rift floor fault-controlled hot springs around the shores of lakes Shala and Langano. This might be related to deeper thermal source that passed through acidic volcanics. In contrast to rift hot springs, the highland hot springs have lesser TDS. Almost all hot springs and hot thermal borehole have Na-HCO₃ waters in the entire basin. It can be concluded that Na is inherently associated with the acidic volcanics and thermal systems.

With the exception of fault-controlled groundwater system east of lake Ziway and north of Langano, all rift waters have higher TDS dominated by Na and HCO₃. They have also higher Cl and fluoride (F). The most dramatic difference between highland and rift waters is the F content. The rift floor is known by exceptionally high F, which made the water unusable for drinking purposes (Teklehaimanot et al., 1987; Ayenew, 1998).

The F level in groundwater can be controlled by the availability of F-bearing minerals and their leaching from the rock formations serving as a pathway. Temperature also plays an important role. The solubility of F is governed by the solubility of its least soluble compound, which in the case is calcium fluoride (CaF₂). Higher dissolved calcium in the groundwater brings about lower level of F (Hem, 1970). Hence, any increase in the calcium content must be compensated for by the precipitation of CaF₂.

In this study attempt is made to calculate the saturation indices of fluorite and calcite to ascertain the mechanism and distribution of fluoride. Based on the hydrochemical model calculations scatter plot is drawn indicating the equilibrium conditions. Generally water samples with low salinity and TDS are sub-saturated with respect to fluorite (Figure 4). These waters are not in equilibrium with the mineral phase fluorite (CaF₂). A trend is observed that higher mineralized waters are saturated with respect to fluorite (Table 2). Fluoride concentrations are controlled by the solubility of the mineral phase fluorite. Water samples with higher F concentrations (greater than 0.2 meq/l) have saturation index values around zero; the majority of them are plotted between -1 and 1. These water samples are close to equilibrium with the mineral phase of fluorite. Fluoride is closely related to higher TDS, alkalinity, sodium and pH. However, waters with high calcium are all with very low fluoride (<1.5 mg/l) characterizing the highland flushed fresh waters.

The Ca and Mg concentration in the deep thermal waters is very low. As a result of steam separation some

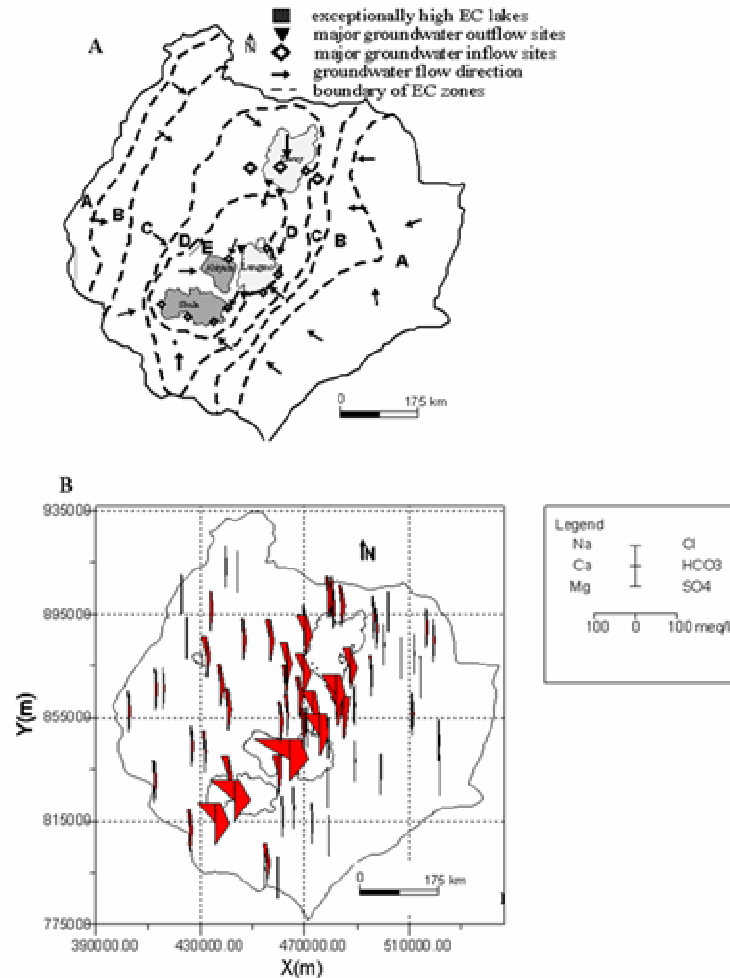


Figure 5. Hydrochemical maps (A = EC distribution in $\mu\text{S/cm}$, B = Stiff diagram for selected borehole samples). EC Zones or classes from A – E represent: A = < 150 $\mu\text{S/cm}$; B = 150-500 $\mu\text{S/cm}$; C = 500-1000 $\mu\text{S/cm}$; D = 1000-1500 $\mu\text{S/cm}$; E = 1500-10000 $\mu\text{S/cm}$.

wells have highest Ca and moderate Mg (Gizaw, 1996). Low Ca and high F concentrations in thermal waters are also favored by low salinity, high CO₂ and temperature (Ellis and Mahon, 1977). The thermal waters are close to calcite (CaCO₃) saturation and the common Ca and Mg-bearing minerals are calcite and epidote and chlorite, respectively (Gizaw, 1996). The high solubility product of calcite, favors its precipitation over fluorite.

Koga (in UNDP, 1973) determined the F concentrations in various sodium bicarbonate solutions and concluded that HCO₃ concentration can considerably affect the extraction of F from rocks. If the pH of the groundwater remains reasonably constant, any increase or decrease in HCO₃ concentration/activity will be accompanied by a corresponding increase or decrease in the concentration/activity of F ions. The waters at the center of the basin have very high F and HCO₃, which are positively correlated with each other, as presented in Table 2.

The lake waters plot in two separate positions on the

Piper diagram. The first group represents the fresh lake Ziway. In this case the dominant cation is Na followed by Ca and Mg, and the dominant anion is HCO₃. The second group represents lakes Langano, Abiyata and Shala. In these waters the dominant cation is Na and the dominant anion is HCO₃ followed by chlorine. They have relatively very high sodium and bicarbonate concentration. The lake Ziway waters affect the groundwaters between Abiyata and Ziway. Boreholes close to the lakes display more or less similar hydrochemical signature. Independent isotopic studies suggested that groundwater migrates from Ziway area to Abiyata and finally all converges to lake Shala located at the lowest topographic position (Ayenew, 2003).

The wide spatial variations of the hydrochemistry of natural waters can be observed from electrical conductivity (EC) and Stiff pattern maps (Figure 5). Stiff patterns visually allows us to trace the flow paths (Stiff, 1951). The stiff plot shows the clear differences in the concentration

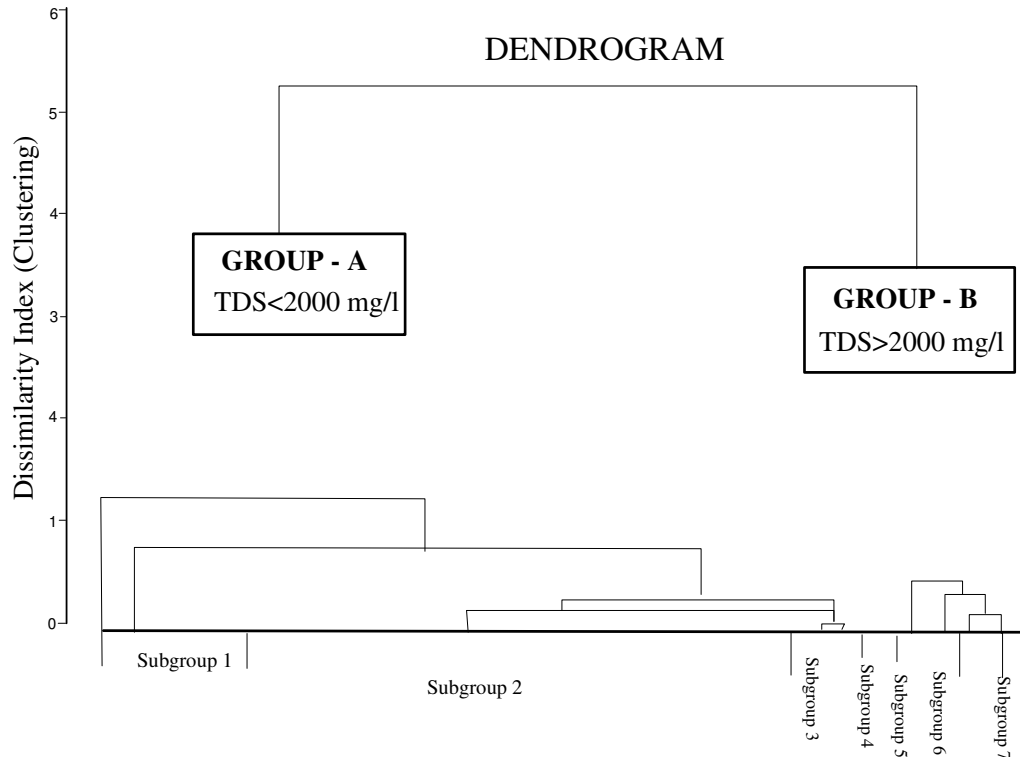


Figure 6. Dendrogram of the Q-mode hierarchical cluster analysis (HCA). The “phenon line” is chosen at dissimilarity index = 0.25 to select the 7 subgroups.

of different ions between the highland and rift waters. The rift waters have distinctly higher EC with very high Na and HCO_3 . The highland waters have low EC and are Ca-Mg- HCO_3 type. In the escarpment the concentration of Na and Cl rises slightly.

The increasing trend in the size of the Stiff symbol from the northwestern highland towards lake Ziway indicates the chemical evolution from fresh water to more saline groundwater along the groundwater flow path. Particularly the alkaline earth ionic concentration increases towards the rift. The same trend is also evident from the western and southwestern escarpment areas all the way to lakes Abiyata and Shala. The sizes of the Stiff symbols are almost uniform on the eastern highlands and escarpments and in the rift east of Ziway where fracture controlled fresh water exists (Ayenew, 1998). These iso-concentration symbols in these areas are aligned parallel to the NNE-SSW and the N-S striking WFB possibly including the adjoining faults close to lakes Langanu and Shala where relatively less concentrated hot springs emanate. In the rift valley the higher EC and concentration of Na and HCO_3 is clearly evident.

Discussion on Q-mode hierarchical cluster analysis

Nine variables (Ca, Mg, Na, K, HCO_3 , CO_3 , Cl, SO_4 and TDS) and 126 water samples were considered for the cluster analysis. The Q-mode clustering resulted in two

major water groups (Groups A and B) and seven subgroups (SB), which were selected from the dendrogram or tree diagram of the cluster analysis (Figure 6). The subgroups were chosen from the dendrogram using a 0.25 index of dissimilarity. Because, at this index the seven subgroups that resulted were very clearly distinguishable in terms of their hydrogeological and hydrochemical variables.

The inclusion of TDS in the cluster analysis separated clearly the highland and rift waters. Even within the rift floor, the most important fault controlled waters are separated from the groundwaters confined in the dominantly lacustrine sediments based on TDS. The two major groups are distinguished by their TDS. Group-A waters have TDS less than 2000 mg/l. Group-B waters have TDS greater than 2000 mg/l. Group-A waters have three subgroups and Group-B waters have four subgroups. The seven subgroups have members from 91 wells, 19 cold springs, 12 hot springs, 5 thermal gradient wells (shallow hot wells) and 7 very deep Aluto geothermal field wells. Thermal gradient well water (TW6) forms a single subgroup.

The samples clustered under each subgroup and the average values for each of the physico-chemical composition are presented in Table 3. The average values for each of the composition of the subgroups produced by the HCA analysis reveal trends between them and they are the basis for the distinction of the subgroups. The

Table 3. Mean concentrations (unit in meq/l) for groups and subgroups derived from HCA.

Group	Subgroup	Ca	Mg	Na	K	CO ₃	HCO ₃	Cl	SO ₄	TDS
A	1 ⁷	0.98	0.42	1.55	0.25	0.15	3.35	0.44	0.08	332
	2 ⁷⁶	0.43	0.26	3.86	0.31	0.07	4.57	0.49	0.09	475
	3 ¹¹	0.14	0.06	15.61	1.37	0.65	11.78	2.46	0.13	1184
B	4 ³	0.03	0.03	97.51	1.02	6.74	44.48	38.75	0.70	6538
	5 ⁸	0.06	0.03	40.88	2.05	0.12	25.91	13.16	0.76	3351
	6 ³	0.07	0.15	43.60	4.31	1.08	22.18	13.09	3.71	3249
	7 ⁷	0.06	0.02	28.27	1.11	0.26	21.47	2.48	2.99	2441

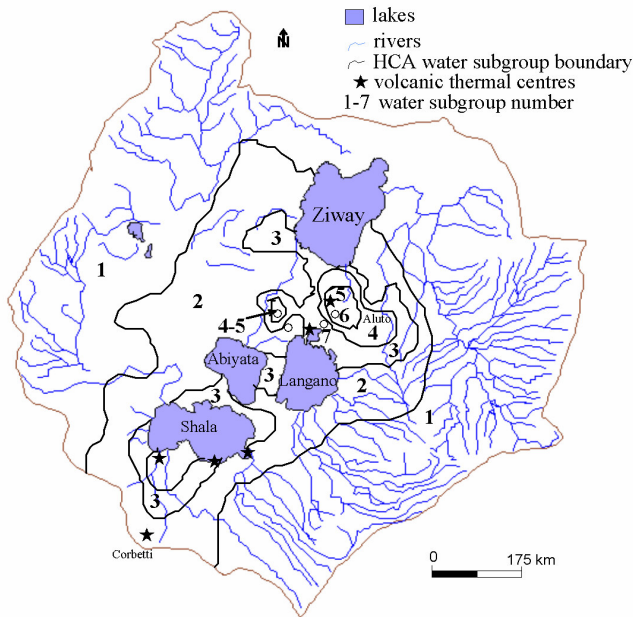


Figure 7. Distribution of hydrochemical facies.

HCA result is consistent with the analysis made on the basis of Piper plots. Most important trends are increase of Na and TDS towards the rift and the reverse in Ca and Mg as one goes down from SB-1 to SB-7. For instance, SB-1 appears to be distinguished from SB-2 by the lower Na value (1.55 meq/l) and higher Ca value (0.98 meq/l); SB-2 differs from SB-3 by higher Na, K, Cl and TDS values and lower Ca value. The good statistical coherence among mean values of the subgroups can be clearly explained in terms of the hydrochemical characterization of groundwater circulations and surface water-groundwater interactions. A detailed account of the localization and their geochemical evolution of these waters is presented in Table 4.

Figure 7 shows the spatial distribution (zonation) of the seven cluster subgroups. The relationship between the statistically defined clusters of samples and geographic location was prepared by plotting subgroup values for each sample. The seven subgroups are separated geographically, as well as physiographically with good correspondence between spatial locations and the HCA results. Samples that belong to the same subgroup are

located in close proximity to one another suggesting more or less the same hydrogeochemical processes (evolution) and/or flow paths. Subgroups which have small number of samples are located as a point data on the map. The high degree of spatial and statistical coherence suggests that the changes between the principal hydrochemical facies define the hydrochemical evolution of water in the basin across the rift valley with distinct spatial patterns representing the rift, escarpment and highlands.

Several of the samples in SB-1 are clustered on the highlands and escarpment edges. Some samples of this subgroup are located in the highly faulted area north of lake Langano. The map also shows that the majority of SB-2 waters are located in the rift. Some members of this subgroup which have relatively higher TDS than SB-1 samples but spatially found on the eastern and western escarpment plotted as point data. All other subgroups are confined within the rift floor.

Most of the samples of SB-1 are located above 1750 m.a.s.l. SB-2 samples (transition zone waters) are mostly located below 1750 m.a.s.l. SB-3 samples (discharge area waters) are all located in the rift floor, and specifically between SB-2 and SB-4. SB-4 waters are evolved from SB-3 waters located in the highly faulted eastern half of the rift floor. SB-6 and SB-7 samples are associated with geothermal systems around lakes Langano and Shala representing highly alkaline hot springs and hot wells drilled for geothermal exploration purpose in the Aluto volcanic complex.

The TDS of SB-1 waters are low which indicates that SB-1 is recharge area waters and increases as the water moves towards the rift where SB-2 waters are situated. SB-3 waters have high TDS (average ~1184 mg/l) which increases to the highest TDS of all the subgroups (average = 6538 mg/l). SB-3 and SB-4 are discharge area waters. SB-2 waters are localized in the transitional recharge and discharge areas. Groundwater in the recharge area evolves from dilute Na-Ca-HCO₃ water type (average TDS is = 332 mg/l) to a fresh Na-HCO₃ water (average TDS is = 475 mg/l) to a more concentrated Na-HCO₃ water (average TDS is = 1184 mg/l) to a brackish Na-HCO₃-Cl water (average TDS is = 6538 mg/l) following the groundwater flow path.

Plotting the principal hydrochemical facies on the site map shows that Group 1 waters are mainly located in the

Table 4. Description of water cluster groups (Numbers in the superscript indicate the number of samples of the subgroup).

Subgroup	Description
1	Several of the samples are located on the highlands and the transitional escarpments. They are Na-Ca-HCO ₃ type with low TDS. Most of the highland cold springs have high Ca. Two hot springs associated with faulted areas have high Na and HCO ₃ content in the group. They also have relatively higher Ca as compared to rift hot springs. These hot springs are located in the rift valley at northern bay of lake Langano (Tuffa area). This subgroup represents early stage of geochemical evolution of young meteoric or recharge areas waters.
2	Samples of this subgroup are located in the rift valley and partially in the eastern escarpments with the exception of the hot springs which are located on the western escarpments. These groundwaters fall in the Na-HCO ₃ water types with subordinate Ca and Mg. They represent intermediate rock-water interactions and groundwater residence time. This group represents slight alteration along the flow path from the parent subgroup 1 waters.
3	The samples are located in the rift valley confined near the lakes and on the highly faulted areas. The high TDS groundwaters of this subgroup fall in the more concentrated Na-HCO ₃ type waters. This is probably with further hydrolysis of silicate minerals by subgroup-2 waters. The concentration of Na and Cl increase but Ca becomes very low. The high TDS and the enrichment of Na therefore testify that the thermal and the high TDS groundwaters have undergone a relatively pronounced degree of groundwater chemical evolution with likely contribution of salts from lacustrine deposits.
4	Members of this subgroup are boreholes south of lake Langano, and two hot springs at eastern side of lake Shala. These waters are Na-HCO ₃ -Cl type waters and they can be classified as discharge area waters representing mixed origin with higher TDS (~6538 mg/l) and likely contributions of salts from the lacustrine deposits.
5	Subgroup-5 waters contains 1 borehole south of lake Shala , 4 deep geothermal wells at the side of Aluto volcano, and hot springs southwest of lake Shala and north of lake Langano. These waters are Na-HCO ₃ -Cl type waters with high Cl. These waters can be from deep system. Ellis and Mahon, 1977 indicate that high Cl concentrations are usually associated with high temperatures. However, high chloride can also be in part contributed from the lacustrine sediments.
6	They represent two geothermal wells and one hot springs located north of lake Langano. Subgroup-6 waters fall in the Na-HCO ₃ -Cl type waters on the piper plot. They have relatively high K and SO ₄ . The presence of higher SO ₄ indicates contributions from deeper geothermal sources and/or local lacustrine sediments.
7	This subgroup contains 4 thermal gradient wells and 1 hot springs north of Langano, and two dug wells. They are more or less similar to the deep thermal waters of subgroup-5 and 6. The difference is that they contain relatively high Na and SO ₄ . The high SO ₄ content of the shallow wells is certainly related to ionic enrichment from the lacustrine sediments on the Bulbula plain southwest of lake Ziway.

highlands and escarpments. Group 1 cold springs (average TDS is 200 mg/l) reflect short groundwater flow paths at shallow depths. Recharge to these springs probably occurs via fault and/or fracture controlled shallow groundwater flow paths. The low TDS (dilute) cold spring waters of Group 2 waters in the rift floor indicates the occurrence of local recharge through faults.

The dominance of HCO₃ decreases as one goes from the highlands to the rift with exception of lake waters. On the contrary the Cl and SO₄ content increases rift wards. Lake Ziway waters plotted near the subgroup-1 (recharge area) waters which means they have similar ionic proportion indicating that SB-1 waters are the major source waters for lake Ziway through the two major feeder rivers of Katar and Meki. The low-lying lakes Abiyata, Langano and Shala have ionic proportions similar to the SB-3 and SB-4 waters (discharge area waters). The thermal waters of SB-5 and SB-6 waters (geothermal well and hot spring waters) resemble the hydrochemical signature of lakes Shala and Langano, which both are fed by numerous hot springs.

Conclusions

The conventional hydrochemical data analysis and the Q-mode hierarchical cluster analysis revealed the existence of different hydrochemical facies corresponding to various hydrogeological regimens across the rift valley. It also demonstrated the groundwater flow pattern in the different physiographic regions and the interaction of the rift lakes with the groundwater with different hydrochemical signature.

The most important distinguishing feature of the rift and highland waters is the TDS and the concentration of major ions including fluoride. The rift waters are distinctly Na-HCO₃ type with very high TDS and fluoride. On the contrary highland waters are Ca-Mg-HCO₃ type with very low TDS. Locally highland thermal springs with higher TDS display exceptional hydrochemical signatures. In few localities of the rift fresh fault-controlled highland waters were identified.

The evolution of the groundwater across the rift can be clearly identified along flow paths. The water tends to

evolve from low TDS and Ca-Mg-HCO₃ type recharge area highland waters to Na-Ca-Mg-HCO₃ type with moderate TDS in the escarpment and finally to a highly concentrated Na-HCO₃ and Na -HCO₃ -Cl type rift waters.

The influence of the rift lakes on the groundwater can be observed by comparing the hydrochemical signature of the lakes and wells in the vicinity. The majority of waters from the fresh lake Ziway fall in Na-Ca-Mg-HCO₃ type waters, which are more or less similar to the highlands and escarpment ground waters. The majority of water samples from the alkaline lakes Abiyata, Langanu and Shala are Na-HCO₃-Cl type displaying similar signature in some ions and TDS as discharge area waters or hot springs feeding the alkaline lakes.

The statistical cluster analysis defined two major water groups and seven subgroups by considering nine hydrochemical variables. The cluster analysis clearly demonstrated that the hydrochemical regiment of the highland and the rift is distinctly different with intermediate composition in the transitional escarpment. These classifications enabled to map water groups within and across the rift displaying the close association of hydrochemical facies and physiographic zones.

The high spatial variations of major cations and anions follows systematic trend along topographic and hydraulic gradients. The cluster analysis and mapping of water groups on the base map shows that there is a general groundwater flow and evolution from SB-1 → SB-2 → SB-3 then to SB-4.

The assessment of the different hydrochemical facies, their spatial variability in relation to the groundwater dynamics certainly plays important role in finding and developing good quality groundwater that can be used for various purposes.

ACKNOWLEDGMENTS

The Department of Earth Sciences of Addis Ababa University is highly acknowledged for the logistic support and providing laboratory facilities. Part of this work was supported by the French government-supported MAWARI project. The authors are also indebted to the Alexander von Humboldt Foundation for providing a fellowship grant for the first author to do part of the research at the Department of Applied Hydrogeology, Ruhr University of Bochum (Germany).

REFERENCES

- Adams S, Tredoux G, Harris C, Titus R, Pietersen K (2001). Hydrochemical characteristics of aquifers near Sutherland in the Western Karoo, South Africa. *J. Hydrol.* 24: 91–103.
- Ayenew A (1998). The hydrogeological system of the lake district basin, Central Main Ethiopian Rift. PhD thesis, Free University of Amsterdam. p. 259.
- Ayenew A (2001). Numerical groundwater flow modelling of the central Main Ethiopian Rift lakes basin. *SINET: Ethiop. J. Sci.* 24(2):167–184.
- Ayenew A (2003). Environmental isotope-based integrated hydro-geological study of some Ethiopian rift lakes. *J. Radio-analytical and Nuclear Chemistry.* 257(1): 11–16.
- Ayenew A (2005). Major ions composition of the groundwater and surface water systems and their geological and geochemical controls in the Ethiopian volcanic terrain. *SINET: Ethiop. J. Sci.* 28(2): 0379–2897.
- Ayenew T, Legesse D (2007). The changing face of the Ethiopian rift lakes: Call of the time. *Lakes and reservoirs: Research and Management.* 12: 149–165.
- Chernet T, Travi Y, Valles V (2001). Mechanism of degradation of the quality of natural water in the lakes region of the Ethiopian Rift Valley. *Wat. Res.* 35(12): 2819–2832.
- Craig H, Lupton JE, Horowitz RM (1977). Isotope geochemistry and hydrology of geothermal-waters in the Ethiopian Rift Valley. *Scripps Inst. of Oceanography.* p. 160.
- Darling WG, Gizaw B, Arusei MK (1996). Lake-groundwater relationships and fluid-rock interaction in the African rift valley: Isotopic evidence. *J. Afr. Earth Sci.* 22: 423–431.
- Di Paola GM (1972). The Ethiopian Rift Valley (between 7° 00' and 8° 40' lat. north). *Bulletin of Vulcanology* 36: 517–560.
- Edmunds WM, Smedley P (2000). Residence time indicators in groundwater: the East Midlands Triassic sandstone aquifer. *J. Applied Geochem.* 15: 737–752.
- Ellis AJ, Mahon WAJ (1977). *Chemistry and Geothermal Systems.* Academic Press.
- Fournier RO, Truesdell AH (1970). Chemical indicators of subsurface temperature applied to hot spring waters of Yellowstone National Park, Wyoming, USA. *Geothermics Special Issue* 2: 529–535.
- Gasse F (1980). Late Quaternary changes in the lake levels and diatom assemblages on the southeastern margin of the Sahara. *Paleoecol. Afri.* 11:117-134.
- Gasse F, Street FA (1978). Late Quaternary lake-level fluctuations and environments of the northern Rift Valley and Afar region (Ethiopia and Djibouti). *Palaeogeogr. Palaeoclimatol. Palaeoecol.* 24: 279–325.
- Gizaw B (1996). The origin of high bicarbonate and fluoride concentrations in waters of the Main Ethiopian Rift Valley, East African Rift system. *J. Afr. Earth Sci.* 2: 391–402.
- Güler C, Thyne GD, McCray JE, Turner AK (2002). Evaluation of graphical and multivariate statistical methods for classification of water chemistry data. *Hydrogeol. J.* 10(4): 455–474.
- Güler C, Thyne GD (2003). Hydrologic and geologic factors controlling surface and groundwater chemistry in Indian Wells-Owens Valley area, south-eastern California, USA. *J. Hydrology.* 285(1-4): 177-198.
- Hem JD (1970). Study and interpretation of the chemical characteristics of natural waters, US. Geol. Surv. Water Supply Paper 1473: 363
- Kebede S, Travi Y, Alemayehu T, Ayenew T (2005). Groundwater Recharge, Circulation and geochemical Evolution in the source region of the Blue Nile river, Ethiopia. *Appl. Geochem.* 20(9): 1658-1676.
- McKenzie J, Siegel D, Patterson W, McKenzie J (2001). A geochemical survey of spring water from the main Ethiopian Rift Valley, southern Ethiopia: implications for well head protection. *Hydrogeol. J.* 9: 265-272.
- Meng SX, Maynard JB (2001). Use of statistical analysis to formulate conceptual models of geochemical behaviour: water chemical data from the Botucatu aquifer in Sa'õ Paulo state, Brazil. *J. Hydrol.* 250: 78–97.
- Merla G, Abbate E, Azzaroli A, Bruni P, Canuti P, Fazzuoli M, Sagri M, Tacconi P (1979). A Geological map of Ethiopia and Somalia, and comment. CNR, Firenze.
- Mohr P (1983). Ethiopian flood basalt province. *Nature* 303: 577–584.
- Parkhurst DL, Appelo CAJ (1999). PHREEQC a computer program for speciation, batch reaction, one-dimensional transport, and inverse geochemical calculations. United States Geological Survey (USGS) water resources investigation report. 99-4259. 312 pp.
- Plummer L, Busby J, Lee R, Hanshaw B (1990). Geochemical modelling of the Madison aquifer in parts of Montana, Wyoming, and South Dakota. *Water Resour. Res.* 26: 1981–2014.
- Stiff HA (1951). The interpretation of chemical water analysis by means of patterns: *Journal of Petroleum Technology,* 3(10): 15-17.
- Street FA (1979). Late Quaternary lakes in the Ziway-Shala Basin, Southern Ethiopia. (UK). PhD thesis [Quaternaire: STR-80.094].

Teklehaimanot R, Fekadu A, Bushra B (1987). Endemic fluorosis in the Ethiopian Rift Valley. *Trop. Geogr. Medicine* 39: 209-217.

UNDP (1973). Investigation of geothermal resources for power development: Geology, geochemistry and hydrology of hot springs of the East African Rift System within Ethiopia (with maps), New York.

Woldegabriel G, Aronson JL, Walter RC (1990). Geology, geochronology, and rift basin development in central sector of the Main Ethiopian Rift. *Geological Society of America Bulletin*, 102 (1990): 439-458. [B34.022].